

Tracking of MPP for three-level neutral-point-clamped qZ-source off-grid inverter in solar applications

Carlos Roncero-Clemente¹, Oleksandr Husev^{2,3}, Víctor Miñambres-Marcos¹, Enrique Romero-Cadaval¹, Serhii Stepenko^{2,3} and Dmitri Vinnikov³

¹Power Electrical and Electronics Systems (PE&ES), University of Extremadura, Spain

²Dept. of Industrial Electronics, Chernihiv State Technological University, Ukraine

³Dept. of Electrical Engineering, Tallinn, Estonia

Abstract: This research work analyzes the most popular maximum power point tracking algorithms for an off-grid photovoltaic system based on three-level neutral-point-clamped quasi-z-source inverter topology to transfer the maximum power to the loads or storage systems. Classical methods, such as dP/dV feedback, perturb and observe method and incremental conductance, have been adapted for this novel topology and tested by simulation in SimPowerSystem from Matlab/Simulink. All of them use the shoot-through duty cycle as a control variable in dynamic conditions of irradiance to generate the reference shoot-through duty cycle in the modulation technique. In the studied case the power converter is feeding a pure resistive load in all the methods compared. Finally, the dP/dV method has been implemented in the control system of an experimental prototype and verified in a real photovoltaic system.

Keywords: Multi-level inverter, solar energy, pulse width modulation converters, neutral-point-clamped inverter, quasi-z-source inverter, shoot-through, maximum power point tracking, photovoltaic system

Sledenje točke največje moči s trinivojskim NPC quasi-Z-source neomrežnim razsmernikom v solarnih aplikacijah

Izveček: Raziskava opisuje najbolj popularen algoritem sledenja točke največje moči za neomrežne fotonapetostne sisteme na osnovi trinivojskih NPC quasi-z-source topologij razsmernika za prenašanje največje moči v bremena ali shranjevalnike. Klasične metode, kot so dP/dV, motilno opazovalne metode in inkrementalna prevodnost, so bile prirejene za novo topologijo in preizkušene s simulacijskimi orodji SimPowerSystem in Matlab/Simulink. Za generiranje referenčnega kratkostičnega vklopnega razmerja v tehniki modularanja vse metode za kontrolni parameter v dinamičnih razmerah sevanja uporabljajo kratkostično vklopno razmerje. V raziskavah je v vseh primerih razsmernik napajal čisto uporovno breme. Končno se je dP/dV metoda vgradila v kontrolni sistem prototipa in se preverila na realnem fotonapetostnem sistemu.

Ključne besede: večnivojski razsmernik, solarna energija, pretvornik s pulzno širinsko modulacijo, NPC, quasi-z-source razsmernik, slednje točke največje moči, fotonapetostni sistem

* Corresponding Author's e-mail: croncero@peandes.net

1 Introduction

Today's power electrical system scenario differs essentially from the traditional configuration. Several factors such as increased electrical consumption, electricity market liberalization, the need to reduce pollution and

CO₂ emissions and technological advancement are boosting the distributed generation (DG).

Photovoltaic solar energy is one of the most relevant distributed energy resources in this new scenario [1]. Due to increased use of this technology, several regu-

lations [2] have been established in order to manage the photovoltaic plant inverters. These regulations stipulate that the inverters are to provide support and stability during grid fault events and injected reactive power is necessary in order to restore the voltage at the point of common coupling (PCC), especially when voltage sag occurs.

This energy can output only DC voltage, therefore an inverter interface has to be used, which requires reduced cost and increased reliability inverter topologies. Among inverter topologies, the three-level neutral-point-clamped (3L-NPC) inverter has several advantages over the two-level voltage source inverter, such as lower semiconductor voltage stress, lower required blocking voltage capability, decreased dv/dt , better harmonic performance, soft switching possibilities without additional components, higher switching frequency due to lower switching losses, and balanced neutral-point voltage. As a drawback, it has two additional clamping diodes per phase-leg and more controlled semiconductor switches per branch. The 3L-NPC can normally perform only the voltage buck operation. In order to ensure voltage boost operation, an additional DC/DC boost converter should be used in the input stage [3]-[5]. It is necessary because in solar energy application, a wide range regulation capability of the input voltage is required due to its dependence on irradiance (W) and temperature (T).

To obtain buck and boost performance in a single stage, the focus is turned to a quasi-Z-source inverter (qZSI). The qZSI was introduced in [6] and it can buck and boost the DC-link voltage in a single stage without additional switches.

The qZSI can boost the input voltage by introducing a special shoot-through switching state, which is the simultaneous conduction (cross conduction) of both switches of the same phase leg of the inverter. In addition, the qZSI has a continuous mode input current (input current never drops to zero), which makes it especially suitable for renewable energy sources (e.g. fuel cells, solar energy, wind energy).

A new qZSI topology was proposed and described in [7]. It is a combination of the qZSI and the 3L-NPC inverter. The three-level neutral-point-clamped quasi-z-source inverter (3L-NPC qZSI) has advantages of both of these topologies.

Since the mentioned topology is rather new, in all previous studies the 3L-NPC qZSI was considered as an off-grid system [7]-[10]. To be connected to the electrical grid, a wide range of conditions should be considered

(synchronization with the grid voltage, MPPT, anti-islanding methods, reactive power control, etc).

This paper discusses three MPPT algorithms (dp/dV feedback, perturb and observe method and incremental conductance) by simulation that can be used in this topology, using the shoot-through duty cycle as a control variable. In our experimental investigation one of the algorithms was verified in a real photovoltaic system.

2 System description

Fig.1 shows the photovoltaic conversion system each stage of which will be explained in this section.

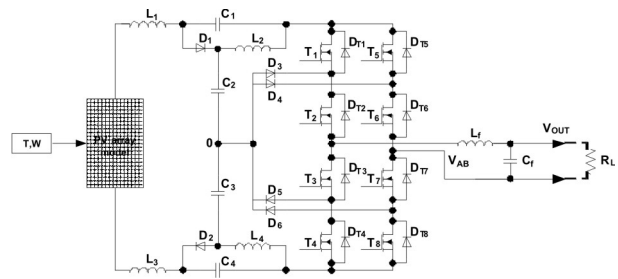


Figure1: Off-grid photovoltaic conversion system based on the 3L-NPC qZSI.

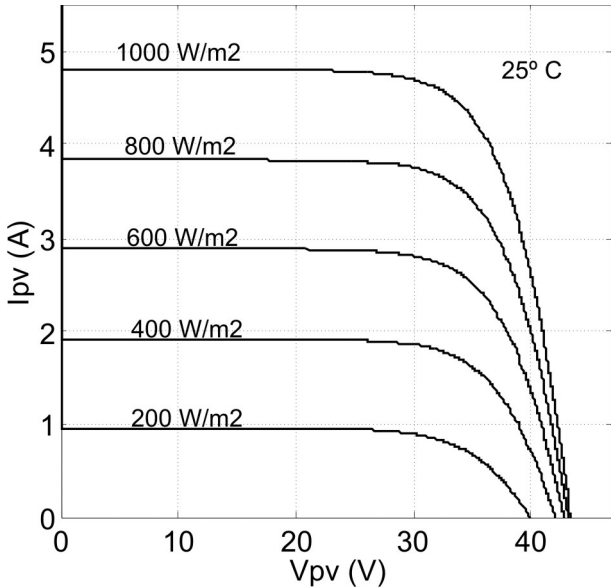
2.1 PV Array Model

Solar panels provide a limited voltage and current following an exponential I-V curve.

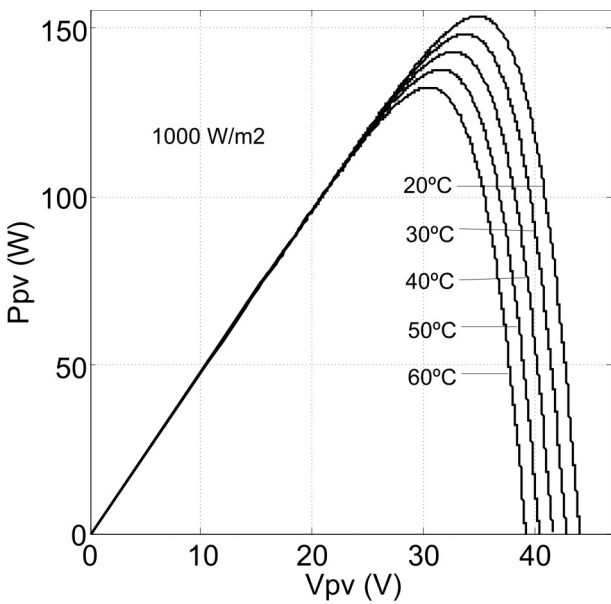
Several models have been proposed for solar panel simulation in the literature [11]-[15]. Most of them model the solar cell as an electrical equivalent circuit where such parameters as junction resistor between P-N unions, the contact resistor between cells and metal parts (R_c) and the resistor for shunt currents (R_{sh}) are needed. In [11-13], even the diode factor and the effective cell area are necessary. These parameters are not provided by the solar panel manufacturers in datasheets, which makes it difficult for engineers and users to apply these models.

Due to these reasons, a mathematical model based on I-V exponential curves and parameters provided by manufacturers in a datasheet was used to simulate the PV array. Mathematical foundation is detailed in [16]. By means of this model and the appropriate series-parallel association of modules, any PV array could be simulated. The family of I-V and P-V curves simulated in different conditions of temperature (T) and irradiance (W) for the case of solar panel Shell SP150-P [17] is shown

in Fig. 2 a) and b). The values of V_{oc} , I_{sc} , I_{MPP} and V_{MPP} were achieved with an error less than 1% in comparison with those provided by the manufacturer.



(a)



(b)

Figure 2: a) I-V family curves changing irradiance. B) P-V family curves changing temperature.

2.2 DC/AC Interface

DC/AC conversion is carried out by means of a single phase 3L-NPC qZSI [7]. This topology presents some particular features, such as continuous input current, higher switching frequency due to lower switching losses, balanced neutral-point voltage and high quality of the output voltage in comparison with traditional

inverters providing benefits in PV conversion applications. One of the most important capabilities of the qZS family of inverters is the possibility of boosting the input voltage by means of shoot-through switching states. This boosting possibility avoids the use of a DC-DC boost converter between the PV array and the inverter to achieve the MPP operation and the control of the system. Passive elements of the qZ network have been calculated according to the method proposed in [9].

2.3 Output Filter and Load

An L-C filter has been chosen to minimize the THD of the output voltage. Filter values have been calculated according to the guidelines in [18]. It is based on current and voltage ripples among others criteria.

To analyze the transferred power from the PV array to the load, a pure resistive load is connected between the branches.

3 Modulation technique

A special sinusoidal pulse-width modulation (SPWM) technique was implemented in order to generate the switching signals of the power converter.

There are two kinds of switching signals to generate separately in ZS and qZS inverters. On the one hand, it is necessary to generate the normal switching signals (S_{Ti}) in order to track the reference signal. On the other hand, the shoot-through states must to be added carefully.

Some requirements must be satisfied when shoot-through states are generated, for instance, the average output voltage should remain unaffected and the shoot-through states have to be uniformly distributed during the whole output voltage period with constant width. These features result in several advantages, such as minimum ripple of the input current, minimum value of the passive elements, reduction of the THD of the output voltage, and gaining of the desired boost factor.

In this work the modulation technique proposed in [10] was used to achieve the aforementioned features. Fig. 3 shows the generation of the normal and shoot-through switching states with this modulation technique and Fig.4. depicts its implementation sketch.

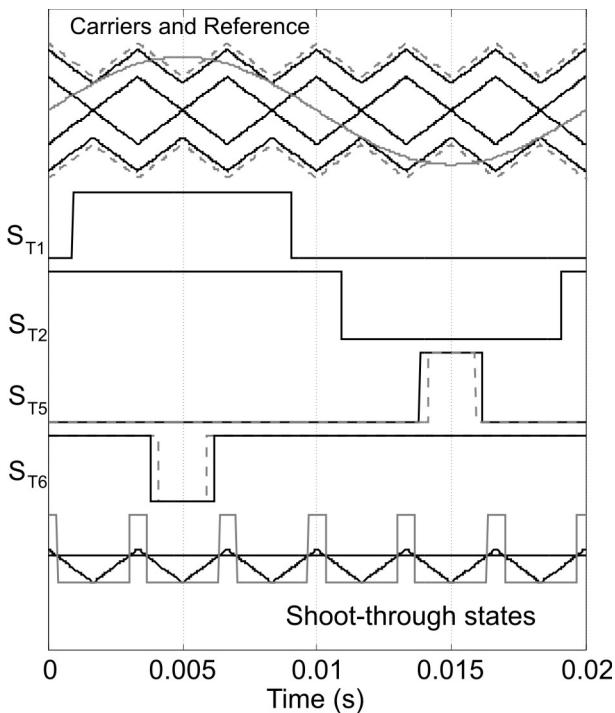


Figure 3: Simulation of the used shoot-through modulation technique.

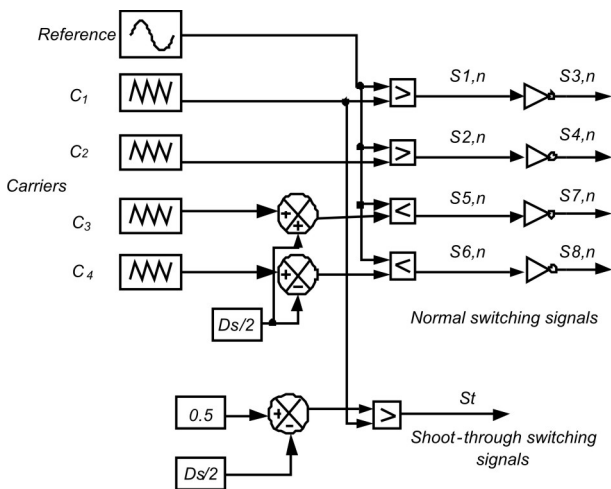


Figure 4: Sketch of the implementation of the modulation technique.

4 MPPT algorithms for 3l-npc qzsi

Tracking the maximum power point (MPP) of a PV array is necessary due to the high cost of solar panels and the dependence of power with W and T [19], being an essential task of PV inverters. In this way, many maximum power point tracker (MPPT) algorithms have been proposed in the literature [20]. Those methods vary in complexity of implementation, sensors required, convergence speed, cost, range of effectiveness and hardware implementation among others [20].

Three most traditional MPPT algorithms are highlighted due to their capabilities: perturb and observe (P&O), incremental conductance (InC) and the method based on DP/dV or dP/dI feedback.

Explained in this section, these MPPT methods have been adapted for the 3L-NPC qZSI topology. All of them work using the shoot-through duty cycle (D_s) as a control variable to track the MPP in dynamic irradiance conditions as well.

Fig. 5 shows the block diagram of the photovoltaic conversion system to be controlled in which the MPPT algorithms have been implemented.

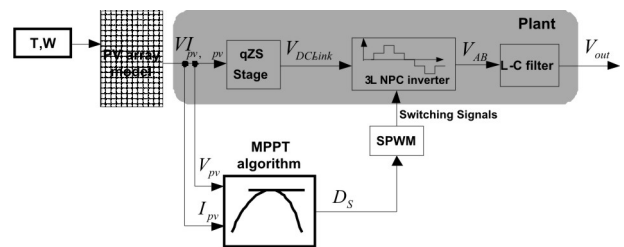


Figure 5: Block diagram of the studied photovoltaic conversion system.

4.1 Method Based on dP/dV Feedback

One way to achieve the MPP operation is to calculate the slope (dP/dV) [21]-[25] of the PV array power curve and feed it back to the converter with any control method to drive such slope to zero.

Depending on the topology and the mode of working of the converter, the slope can be computed in different ways. In our case, a PI controller that adjusts the D_s of the shoot-through modulation technique explained in section III is used to drive the slope to zero. The PI controller was tuned manually, looking for a slow response without error in steady state. This fact is considered to emulate the inertia and the response times of the electrical grid (synchronous machines and conventional power plants) to avoid instabilities and transient non-desired effects [26] when the converter is connected to the grid. Fig. 6 shows the implementation scheme of the MPPT algorithm based on dP/dV feedback for the 3L-NPC qZSI using the D_s as a control variable.

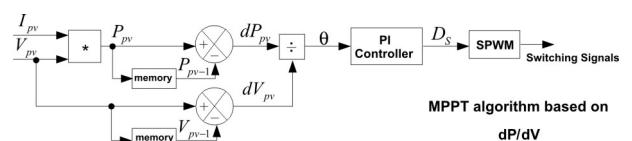


Figure 6: Implementation scheme of dP/dV feedback method.

4.2 Perturb and Observe Method (P&O)

This method [27]-[29] has been used by many researchers in different ways but the idea remains the same. A perturbation in the voltage of the PV array is perturbing the PV array current, resulting in the modification of the PV array power. By means of the increment of the PV voltage when the operation is on the left of the MPP, the PV power is increased and the PV power is decreased if the operation is on the right of the MPP. The same reasoning is possible when the PV voltage is decreased. If one perturbation in one direction produces the increment of the PV power, the next perturbation should be in the same direction and if it is not the case, the perturbation has to be reverse. Table I summarizes the process.

To produce the perturbation in the voltage of the PV array of our case where the DC/AC is converted by a 3L-NPC qZSI, perturbations in the D_s are inserted. The value of this perturbation is equal to 0.005. By means of this process the MPP is reached and the system oscillates around the MPP, as shown in Fig. 7 (points A and B). Fig. 8 depicts a sketch of the implementation of this method.

Table 1: Summary of MPPT Algorithm Based on P&O

Perturbation	Change in Power	Next Perturbation
Positive	Positive	Positive
Positive	Negative	Negative
Negative	Positive	Negative
Negative	Negative	Positive

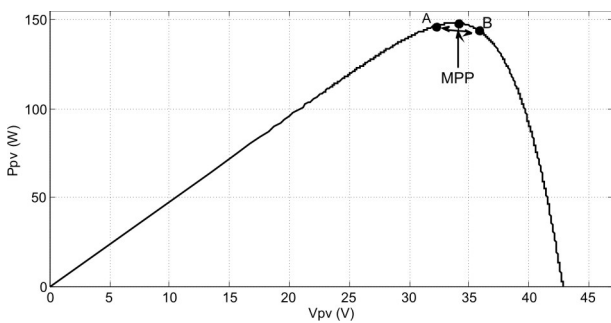


Figure 7: Power operation with the P&O MPPT method.

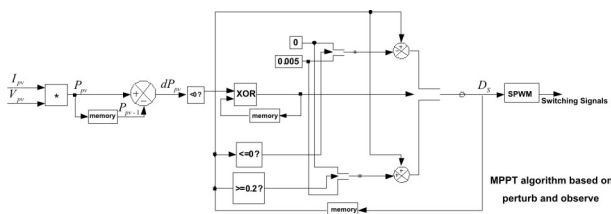


Figure 8: Implementation scheme of the P&O method.

4.3 Incremental Conductance (IncCond)

This method [30]-[31] analyzes the slope of the PV array power curve. This slope is zero at the MPP, positive on the left of the MPP and negative on the right. Thus:

$$\frac{dP}{dV} = \frac{d(IV)}{dV} = I + V \frac{dI}{dV} \cong I + V \frac{dI}{dV} \quad (1)$$

and as a consequence, the incremental conductance $\Delta I/\Delta V$ is equal, greater than or less than $-I/V$ at the MPP, on the left of the MPP and on the right of the MPP, respectively. The MPP can be tracked by comparing the instantaneous conductance (I/V) with the incremental conductance ($\Delta I/\Delta V$) as the flowchart in Fig. 9 shows. In our case by changing D_s , the voltage V_{pv} where the PV array is forced to operate is changed, trying to find the MPP ($\Delta I/\Delta V = -I/V$).

The size of the incremental step (changes inserted in D_s) determines the convergence (velocity and accuracy) of this MPP tracking method. Using larger increments in the control variable, the system will be faster but it will not operate close to the MPP. The step size was designed taking into account the same criteria as the tuning of the PI controller in the method based on dP/dV feedback.

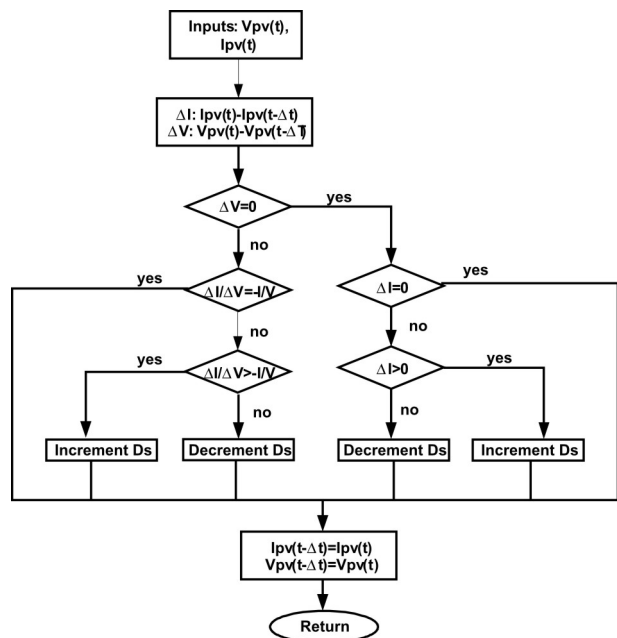


Figure 9: Incremental conductance flowchart.

5 Simulation results

In order to verify the explained MPPT algorithms, a comprehensive simulation study was performed in SimPowerSystems of Matlab/Simulink. Parameters of

the simulation are described in Table II. To analyze the transferred power to the load and the effectiveness of each MPPT method, a smooth step (Fig. 10. a) in the irradiance from 1000 W/m² to 900 W/m² (Fig. 10. b)) in second eight up to sixteen was made while the temperature was maintained constant (25 °C). This action emulates the shadows phenomena. Fig. 11 shows the evolution of the transferred power from the PV array to the load and the evolution of the control variable (D_s) in dynamic conditions by using each MPPT algorithm.

Table 2: Simulation parameters.

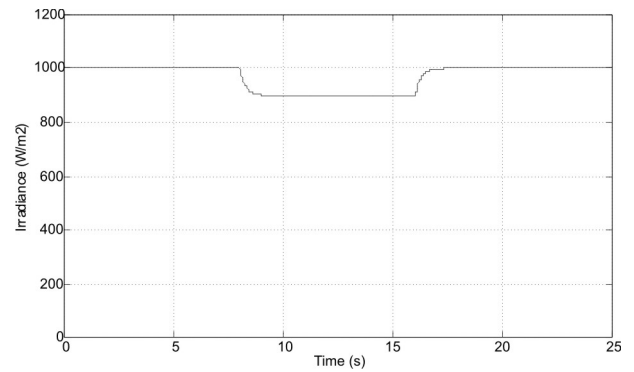
Group	Parameter	Description and unit	Value
PV Array	V_{oc}	Open circuit voltage (V)	43.4
	I_{sc}	Short circuit current (A)	4.8
	I_{MPP}	Maximum power point current (A)	4.4
	V_{MPP}	Maximum power point voltage (V)	34
	N_s	Series connected panel	7
	N_p	Parallel connected panel	1
Passive Elements	Inductors L_1, L_3	(mH)	2.55
	Inductors L_2, L_4	(mH)	0.255
	Capacitor C_1, C_4	(mF)	4
	Capacitor C_2, C_3	(mF)	1.3
	R_{load}	(Ω)	60
	C_{filter}	(μ F)	0.47
	L_{filter}	(mH)	4.4
dP/dV	K_p	Proportional constant of PI controller	0.001
	K_i	Integral constant of PI controller	0.01
P&O		Perturbation size in D_s	0.005
Inc Cond		Perturbation size in D_s	0.005

5.1 Method Based on dP/dV Feedback

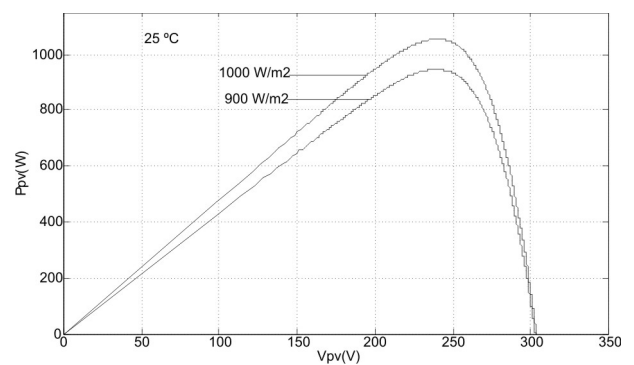
Figs. 11 (a) and 11 (b) show the evolution of the transferred power to the load and the evolution of the D_s when the MPPT algorithm based on dP/dV feedback is working. We can see how the system works in the MPP in each level of irradiance at high accuracy by means of the adjustment of the D_s . It is important to pay attention to some singularities (second sixteen) that could appear when any of the denominators (dV) are equal to zero during the iterative process. The algorithm must be protected against this cause of instability.

5.2 P&O

Figs. 11 (c) and 11 (d) show the evolution of the output power and the D_s in the case of the P&O method. The



(a)



(b)

Figure 10: a) Smooth step applied in the solar system. b) P-V array curves in each level of irradiance during the step.

system again tracks the MPP with accuracy. In this case the system is working around the MPP.

5.3 IncCond

In Figs. 11 (e) and 11 (f) the same variables are shown for the third presented MPPT algorithm. The MPP is also achieved in each level of irradiance using this method.

6 Analytical comparison

In order to compare the exposed MPPT algorithms for a 3L-NPC qZSI, each algorithm is analyzed in this section.

According to the number of required sensors, all of them need the measure of voltage and current of the PV system to track the MPP. There are other traditional algorithms, such as the MPPT algorithm based on the fractional control of V_{oc} and I_{sc} or the method based on the DC link capacitor drop control that only requires the measure of one variable.

In terms of the complexity of the implementation of the analyzed methods, perturbation and observation and incremental conductance are of low complexity level because they are based on simple mathematical

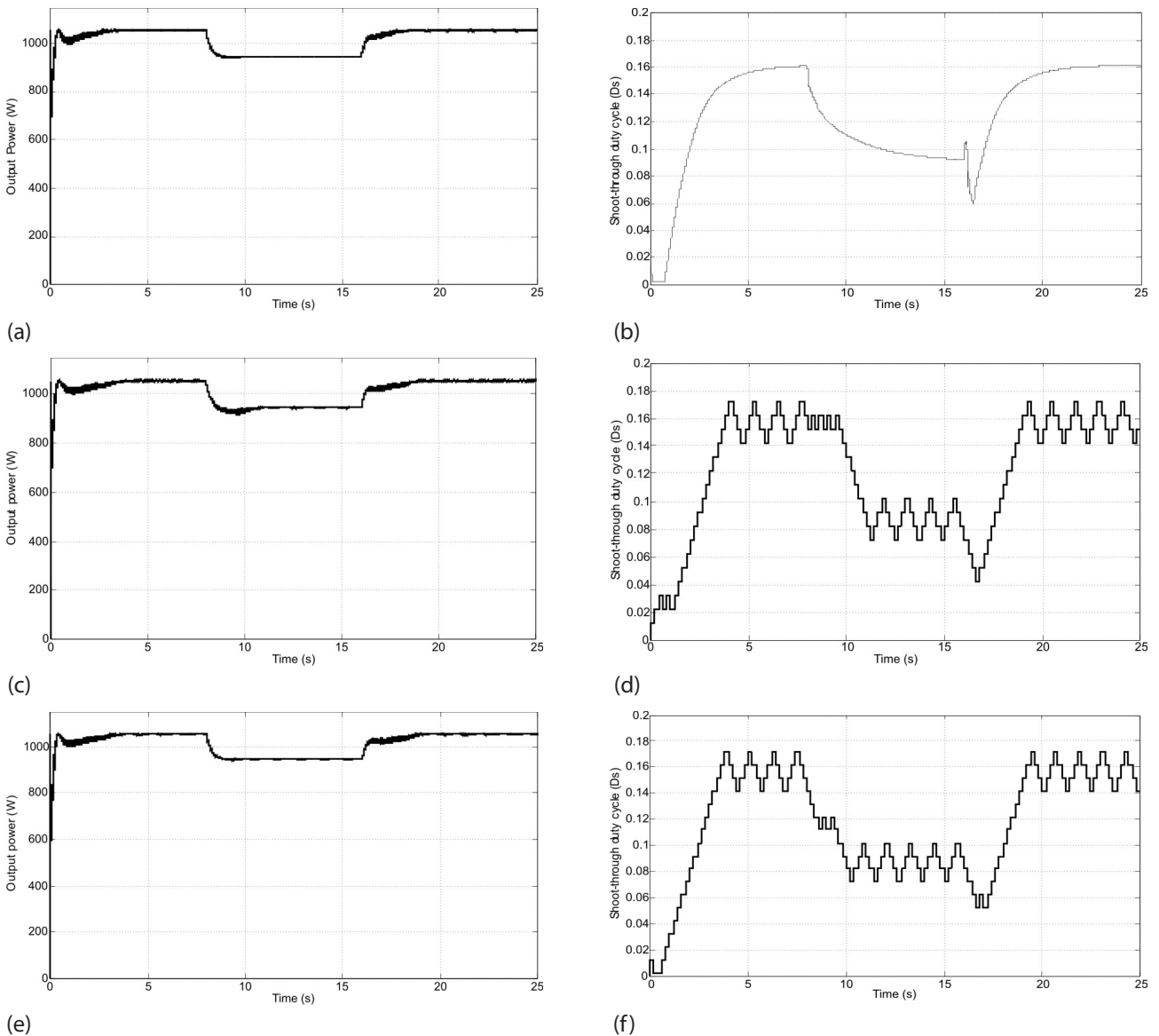


Figure 11: Evolution of transferred power and the evolution of D_s during a step in irradiance in each MPPT algorithm analyzed.

calculations. The MPP tracking algorithm based on dP/dV feedback is more complex due to the necessity to tune a PI controller and the calculation of a division of derivatives in which it is necessary to prevent possible denominators equal to zero.

Another interesting feature is that the three algorithms can be implemented in digital or analogical technologies.

The speed of convergence of each method is quite different. On the one hand, methods based on perturbation and observation and incremental conductance present a variable speed that depends on the size of the step. A larger step produces faster convergence but at the same time, lower accuracy is achieved because the oscillation around the MPP will be larger. On

the other hand, the MPPT algorithm based on dP/dV feedback, in general, has fast convergence. This speed depends on the parameters of the PI controller. In our case, every method has been implemented to find a slow response without error in steady state. This fact is considered to emulate the inertia and the response times of the electrical grid (synchronous machines and conventional power plants) to avoid instabilities and transient non-desired effects when the converter is connected to the grid and some changes in the irradiance or temperature occur. Also, the designed D_s gap of each method has been chosen between 0 and 0.2. Maximum power per used panel is 149.6 W when irradiance and temperature are 1000 W/m^2 and $25 \text{ }^\circ\text{C}$. After the step when irradiance decreases to 900 W/m^2 , the maximum power is 135.17 W per panel. In the studied case where there are seven panels connected in series,

the array maximum power is 1054 W and 946.2 W in each situation. Using any of the studied methods, such values were achieved with accuracy.

7 Experimental results

In this section the experimental tests are explained. The chosen MPPT algorithm to be implemented in the experimental prototype is based on the adapted P&O using D_s as a control variable to introduce the perturbation in the system to reach the MPP. It is due to several reasons: it has a simple structure which allows an easy implementation: only two sensors are needed (to measure I_{pv} and V_{pv}), it can be used for digital or analog systems and it is not necessary to adjust any control system as a PI controller among others.

The converter built is described below. Table III shows the parameters of the experimental prototype of the 3L-NPC qZS inverter, with values of passive elements and also the type of semiconductors indicated. Passive elements were calculated according to [9] and [18], as in simulation studies. Fig. 12 shows the full system.

The control system is implemented in a low cost FPGA Cyclone IV family from Altera company [8]. Flexibility is the main advantage of this option, which allows realizing the shoot-through modulation technique with digital signal processing at high sample frequency. The measurement board is composed of the required current and voltage sensors.

Table 3: System parameters of the experimental prototype.

ELEMENT	VALUE OR MODEL
Control Unit (FPGA)	Cyclone IV EP4CE15E22C8
Driver Chip	ACPL-H312
Power switches	FCH47N60NF
qZS and clamp diodes	CREE C3D20060D
Input DC voltage U_N	220-450 V
Nominal Output AC voltage U_{OUT}	230 V
Capacitance value of the capacitors C_1, C_4	4000 μ F
Capacitance value of the capacitors C_2, C_3	1000 μ F
Inductance value of the inductors $L_1 \dots L_4$	145 μ H
Inductance of the inverter filter inductor L_i	560 μ H

Inductance of the grid filter inductor L_{gi}	200 μ H
Capacitance of the filter capacitor C_f	0.47 μ F
Switching frequency	100 kHz

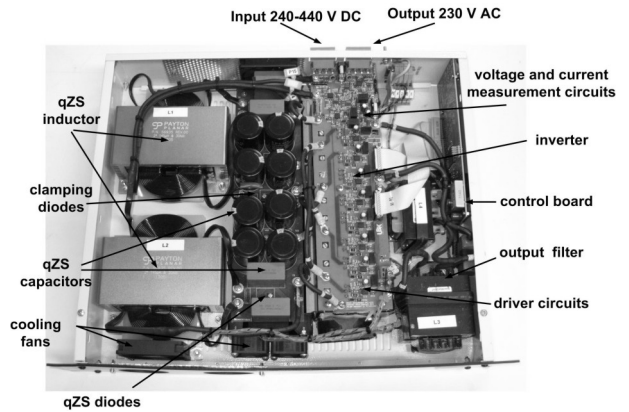


Figure 12: 3L-NPC qZS experimental prototype.

The experimental tests were carried out with a solar array composed of 14 modules LDK 185 D-24 (s), the principal parameters of which in standard conditions of W and T are shown in Table IV. Two strings of 7 serial panels were connected in parallel (2x7 configuration) to obtain a proper input voltage range. The output power is transferred to a pure resistive load.

Table 4: Parameters of module LDK 185 D-24 (s).

Parameters	Value at standard conditions (1000 W/m ² and 25 °C)
Nominal output power (Pmax)	185 W
Voltage at Pmax (Vmpp)	36.9 V
Current at Pmax (Impp)	5.02 A
Open circuit voltage (Voc)	45.1 V
Shot circuit current (Isc)	5.48 A

Fig. 13 shows the obtained results after reaching the maximum power point operation: the output current, output voltage, input PV voltage and input PV current.

Output magnitudes have a high level of quality. Measured total harmonic distortion (THD) with YOKOGAWA DL850 V equipment is 1.5 %. Input PV voltage presents a low frequency ripple at 100 Hz. It is typical of single phase systems. Input PV current presents this low frequency ripple and also ripple at high frequencies due to the switching frequency.

The transferred output power to the load is 1945 W, corresponding to the solar array maximum power at real conditions.

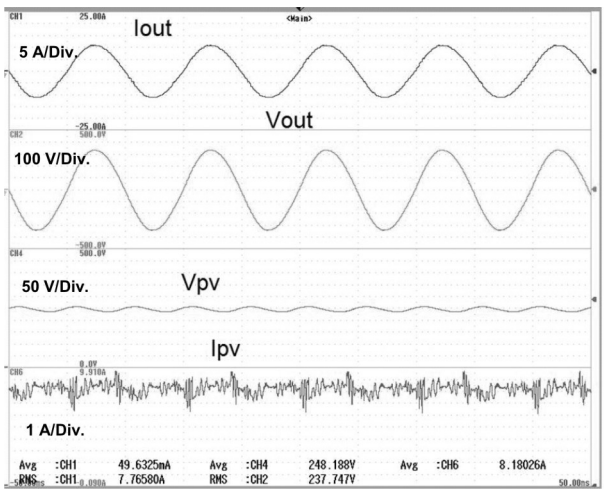


Figure 13: Experimental results at the maximum power point operation. From top to bottom: output current, output voltage, input PV voltage and input PV current.

8 Conclusion

Three traditional maximum power point tracking algorithms (methods based on dP/dV feedback, perturb and observe and incremental conductance) have been compared by means of simulation using SimPowerSystem of Matlab/Simulink. Each method has been adapted for a 3L-NPC qZSI using the shoot-through duty cycle as control variable to reach the MPP operation. Theoretical fundamentals and simulation results have been presented and discussed according to different criteria in order to choose the best solution for a real system. The P&O method, as the best solution, was chosen and implemented in the prototype and validated in a real solar plant.

9 Acknowledgment

The authors would like to thank the Spanish institutions “Ministerio de Economía y Competitividad”, “Junta de Extremadura” and “Fondos FEDER” for their support in this research. The work has been developed under the Project SIDER (TEC2010-19242-C03) and the grant BES-2011-043390. This research work was also partially supported by MOBILITAS Postdoctoral Research Grant (MJD391), by Estonian Ministry of Education and Research (projects SF0140016s11 and B23).

10 References

1. International Energy Agency. Photovoltaic Power Systems Programme, <http://www.iea-pvps.org>. Statistic Reports, 2011.

2. Ministry of Industry, Tourism and Trade of Spain, R.D 1565/2010 Spain, 2010.
3. F. Gao, P. C. Loh, F. Blaabjerg, D. M. Vilathgamuwa, “Dual Z-source inverter with three-level reduced common-mode switching”, IEEE Transactions on industry applications, vol.43, no. 6, pp.1597-1608, 2007.
4. P. C. Loh, S. W. Lim, F. Gao, F. Blaabjerg, “Three-level Z-source inverters using a single LC impedance network”, IEEE Transactions on power electronics, vol. 22, no. 2, pp. 706-711, 2007.
5. Uroš Flisar, Danjel Vončina, Peter Zajec, “Voltage sag independent operation of induction motor based on z-source inverter”. Informacije MIDEM 40(2010) 3, pp. 218-223.
6. Anderson, J.; Peng, F.Z., “Four quasi-Z-Source inverters”, in Proc. of IEEE Power Electronics Specialists Conference PESC’2008, pp. 2743-2749, June 15-19, 2008.
7. Ott, S., Roasto, I., Vinnikov, D., Lehtla, T.: Analytical and Experimental Investigation of Neutral Point Clamped Quasi-Impedance-Source Inverter. Scientific Journal of Riga Technical University, Power and Electrical Engineering, vol.29, pp.113-118 (2011).
8. Stepenko, S., Husev, O., Vinnikov, D., Ivanets, S.: FPGA Control of the Neutral Point Clamped Quasi-Z-Source Inverter. 13th Biennial Baltic Electronics Conference, pp.263-266 (2012)
9. Husev, O., Roncero-Clemente, C., Stepenko, S., Vinnikov, D., Romero-Cadaval, E.: CCM Operation Analysis of the Single-Phase Three-Level Quasi-Z-Source Inverter. The 15th International Power Electronics and Motion Control Conference and Exposition EPE-PEMC 2012 ECCE Europe, pp.DS1b.21-1-DS1b.21-6 (2012)
10. Roncero-Clemente, C., Romero-Cadaval, E., Husev, O., Vinnikov, D.: Simulation Study of Different Modulation Techniques for Three-Level Quasi-Z-Source Inverter. Scientific Journal of Riga Technical University, Power and Electrical Engineering. (2012)
11. A. D. Rajapakse, D. Muthumuni, “Simulation tools for photovoltaic system grid integration studies”. Electric Power & Energy Conference (EPEC), 2009 IEEE. p. 1-5.
12. R.C. Campbell, “A circuit based Photovoltaic Array Model for Power system Studies”. Power Symposium, 2007. NAPS’07. 39th North American. 2007. pp. 97-101.
13. K. Seul- Ki, K. Eung- Sang, A. Jong-Bo. “Modeling and Control of a Grid-connected Wind/PV Hybrid Generation System”. Transmission and Distribution Conference and Exhibition, 2005/2006 IEEE PES. 2006. pp. 1202- 1207.

14. J. Xue, Y. Zhongdong, W. Bingbing, J. Peng. "Design of PV Array Model Based on EMTDC/PSCAD". Power and Energy Engineering Conference, 2009. APPEEC 2009. Asia- Pacific. 2009, pp. 1-5.
15. K. Seul-Ki, J. Jin-Hong, C. Chang-Hee, K. Eung-Sang and A. Jong-Bo. "Modeling and simulation of a grid-connected PV, generation system for electromagnetic transient analysis". Solar Energy, vol. 83, número 5, pp 664-678. May 2009.
16. Carlos Roncero-Clemente, Eva González-Romera, E. Romero-Cadaval, M. Isabel Milanés-Montero, Víctor Miñambres-Marcos. "PSCAD/EMTDC Model for Photovoltaic Modules with MPPT based on Manufacturer Specifications". Compatibility and Power Electronics CPE2013, 8th International Conference-Workshop. Conference Proceeding, ISBN: 978-1-4673-4911-6, pp. 69-74. June 2013.
17. Shell SP150-P. Photovoltaic Solar Module. Product Information Sheet. <http://www.meetegypt.com>
18. Oleksandr Husev, Serhii Stepenko, Carlos Roncero Clemente, Dmitri Vinnikov, Enrique Romero Cadaval. "Output Filter Design for Grid Connected Single Phase Three-Level Quasi-Z-Source Inverter". Compatibility and Power Electronics CPE2013, 8th International Conference-Workshop. Conference Proceeding, ISBN: 978-1-4673-4911-6, pp. 46-51. June 2013.
19. Jože Rakovec, "Exploiting solar energy with photovoltaics". Informacije MIDEM 39 (2009) 4, pp. 213-215.
20. Esram, T., Chapman, P.L., "Comparison of Photovoltaic Array Maximum Power Point Tracking Techniques," IEEE Transactions on Energy Conversion, , vol.22, no.2, pp.439-449, June 2007
21. R. Bhide and S. R. Bhat, "Modular power conditioning unit for photovoltaic applications," in Proc. 23rd Annu. IEEE Power Electron. Spec. Conf., 1992, pp. 708–713.
22. H. Sugimoto and H. Dong, "A new scheme for maximum photovoltaic power tracking control," in Proc. Power Convers. Conf., 1997, pp. 691–696.
23. S. J. Chiang, K. T. Chang, and C. Y. Yen, "Residential photovoltaic energy storage system," IEEE Trans. Ind. Electron., vol. 45, no. 3, pp. 385–394, Jun. 1998.
24. J. A. M. Bleijs and A. Gow, "Fast maximum power point control of current-fed DC–DC converter for photovoltaic arrays," Electron. Lett., vol. 37, pp. 5–6, Jan. 2001.
25. C.-L. Hou, J. Wu, M. Zhang, J.-M. Yang, and J.-P. Li, "Application of adaptive algorithm of solar cell battery charger," in Proc. IEEE Int. Conf. Elect. Utility Deregulation Restruct. Power Technol., 2004, pp. 810–813.
26. F.J Pazos "Operational Experience and Field Tests on Islanding Events Caused by Large Photovoltaic Plants". 21st International Conference on Electricity Distribution. Frankfurt (Alemania). June 2011.
27. O. Wasynczuk, "Dynamic behavior of a class of photovoltaic power systems," IEEE Trans. Power App. Syst., vol. 102, no. 9, pp. 3031–3037, 1983.
28. C. Hua and J. R. Lin, "DSP-based controller application in battery storage of photovoltaic system," in Proc. IEEE IECON 22nd Int. Conf. Ind. Electron., Contr. Instrum., 1996, pp. 1705–1710.
29. M. A. Slonim and L. M. Rahovich, "Maximum power point regulator for 4 kW solar cell array connected through inverter to the AC grid," in Proc. 31st Intersociety Energy Conver. Eng. Conf., 1996, pp. 1669–1672.
30. A. F. Boehringer, "Self-adapting dc converter for solar spacecraft power supply," IEEE Trans. Aerosp. Electron. Syst., vol. AES-4, no. 1, pp. 102–111, Jan. 1968.
31. E. N. Costogue and S. Lindena, "Comparison of candidate solar array maximum power utilization approaches," in Intersociety Energy Conversion Eng. Conf., 1976, pp. 1449–1456.

Arrived: 18. 07. 2013

Accepted: 22. 11. 2013